

## Free-space electro-optic detection of continuous-wave terahertz radiation

Ajay Nahata<sup>a)</sup> and James T. Yardley  
*AlliedSignal, Inc., 101 Columbia Road, Morristown, New Jersey 07962*

Tony F. Heinz  
*Department of Physics and Department of Electrical Engineering, Columbia University,  
New York, New York 10027*

(Received 28 July 1999; accepted for publication 24 August 1999)

We present a scheme for the coherent detection of freely propagating continuous-wave terahertz radiation using electro-optic detection. The terahertz radiation is generated by photomixing two single-mode laser diodes in an antenna fabricated on low-temperature-grown GaAs. This radiation is detected using the electro-optic effect in  $\langle 110 \rangle$  ZnTe. In contrast to typical terahertz detection techniques, this is a frequency-domain measurement that relies on coherent up-conversion of the terahertz field combined with optical homodyning to suppress background noise. © 1999 American Institute of Physics. [S0003-6951(99)00643-9]

The ability to generate continuous-wave (cw) coherent terahertz (THz) radiation using cw laser light has stimulated significant interest in recent years.<sup>1-6</sup> The technique, generally referred to as photomixing, relies on the fact that it is possible to produce optical intensity beats at THz frequencies by mixing two single-mode lasers or by mode beating within a single laser. This amplitude-modulated optical beam is then converted to the base-band frequency by driving a biased photoconductive antenna fabricated on a high-speed semiconductor. A significant advantage of this approach is the ability to create an inexpensive, compact, narrow-linewidth source capable of high-resolution spectroscopy in the far infrared.<sup>3</sup> Other important benefits include the capability for tuning across a wide spectral bandwidth and obtaining THz beams with high spectral brightness.<sup>2,4</sup>

Continuous-wave THz radiation generated from photomixers is typically detected with bolometers. While this approach has proved to be very effective, one must operate bolometers at cryogenic temperatures in order to reduce detection noise. Furthermore, bolometers are square-law detectors, which lose all information about the phase of the THz electric field. Thus, it would be advantageous to develop room-temperature coherent detection techniques. In contrast to time-domain sampling, where noise suppression is achieved by the short "gating" time of the receiver, the detection technique proposed here is a frequency-domain measurement technique that relies on coherent up-conversion of the THz field combined with optical homodyne detection for noise suppression. One approach to this form of detection has recently been demonstrated using photoconductive antennas.<sup>6,7</sup>

In this letter, we demonstrate the application of free-space electro-optic detection<sup>8-10</sup> as an attractive alternate approach for the coherent detection of cw THz radiation. This detection technique has been demonstrated to be a sensitive and extremely fast probe of transient electromagnetic fields.<sup>11</sup> In contrast to the detection of broadband THz radiation, where the trend has been to expand the detection band-

width by decreasing the interaction length in the detection medium, the narrowband nature of the THz radiation in the present case permits long interaction lengths in materials with large optical nonlinearities, thereby increasing the detection sensitivity. For spectroscopic applications, an important issue is the frequency resolution of the system. This resolution is determined by the bandwidth of the THz radiation. Chen *et al.*<sup>3</sup> have shown that the time-integrated linewidth of the photomixed output is  $\sim 90$  MHz when free-running distributed Bragg reflector (DBR) lasers are used. Though not measured in the present study, we expect to achieve similar results.

The experimental setup for generating and detecting THz radiation is shown in Fig. 1. Two single-mode DBR laser diodes operating at a wavelength of  $\sim 850$  nm were combined with a 50/50 beamsplitter. The pump beam, with an average power limited to 35 mW, was used to drive a 100- $\mu\text{m}$ -long dipole emitter fabricated on low-temperature-grown GaAs (LT-GaAs). In order to enhance the THz emission, we fabricated the dipole structure with triangular-shaped tips,<sup>12</sup> which were separated by a 5  $\mu\text{m}$  photoconductive gap. This structure was embedded within a coplanar transmission line composed of 2-cm-long, 10- $\mu\text{m}$ -wide electrodes. The device was antireflection coated to minimize back reflections. The carrier lifetime in the LT-GaAs was measured to be  $\sim 0.5$  ps by time-resolved reflectivity.<sup>13</sup> We modulated the THz beam by applying a 10 kHz square wave to the emitter with an amplitude that varied from +25 to -25 V. This procedure yields a factor of 2 enhancement in the THz signal relative to applying a 25 V dc bias to the emitter and simply chopping the pump beam.

We imaged the cw THz radiation into a 6.7-mm-thick  $\langle 110 \rangle$  ZnTe crystal using two off-axis paraboloidal mirrors. The back face of the crystal was antireflection coated to minimize optical reflections within the crystal. Great care was taken to minimize standing-wave patterns. A pellicle beamsplitter was interposed in the THz beamline to allow for copropagation of the optical probe and THz beams through the electro-optic crystal. The probe beam, which had properties that were identical to the pump beam, was optically bi-

<sup>a)</sup>Electronic mail: [ajay.nahata@alliedsignal.com](mailto:ajay.nahata@alliedsignal.com)

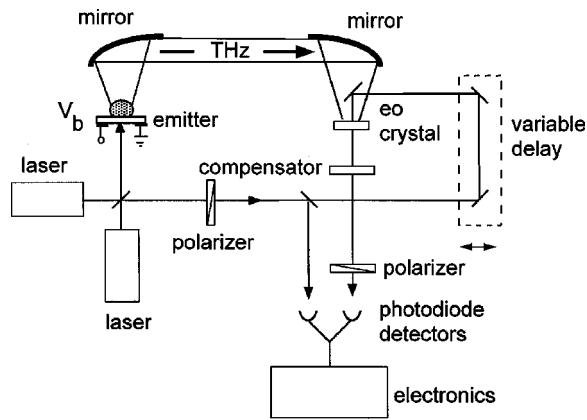


FIG. 1. Schematic drawing of the experimental setup for the generation and detection of freely propagating cw THz radiation. The electro-optic detection was performed in a (110) ZnTe crystal.

used near its null point by a Soleil–Babinet compensator in a crossed polarizer arrangement.<sup>11</sup> Differential detection was used to further improve the sensitivity.

Before turning to the experimental results, we examine the nature of the electro-optic detection technique for the experimental geometry described above and contrast this method with the well-established electro-optic sampling scheme for probing with ultrashort optical pulses. In our experiment, both the pump and probe beams are derived from a pair of single-mode DBR lasers. By combining the output of these two lasers, we may form an optical beam that exhibits amplitude modulation at the desired beat frequency  $\Omega$  in the far infrared. The optical intensity of such a beam is given by  $I_{\text{opt}}(t) = I_{\text{opt}}^0 [A + \cos(\Omega t)]$ , where  $A$  is a constant and we have omitted the spatial dependence for simplicity.

When the optical pump beam excites the dipole emitter, the photoconductance is modulated at the beat frequency by  $I_{\text{opt}}(t)$  and the corresponding base-band radiation is coupled into free space by the antenna. This emission process by photomixing, which has been examined in great detail in earlier studies,<sup>1</sup> produces a cw THz field,  $E_{\text{THz}}(t)$  that is directly proportional to the optical intensity. Therefore, we may write  $E_{\text{THz}}(t) = E_T \cos[\Omega t - \varphi_1]$ , where  $E_T (\propto I_{\text{opt}}^0)$  is the amplitude of the THz field and  $\varphi_1$  is a phase term. The relative phase of the THz beam is related to the optical pathlength  $d_1$  of the pump arm by  $\varphi_1 = \Omega d_1 / c$ , where  $c$  is the speed of light.

The detection of  $E_{\text{THz}}(t)$  the electro-optic (EO) crystal, through which the probe and THz beams propagate collinearly. In an ideal electro-optic measurement performed in the linear response regime, the effective electro-optic signal  $\Delta I_{\text{EO}}(t)$  is proportional to the product of the optical probe intensity and the THz field amplitude:

$$\Delta I_{\text{EO}}(t) \propto I_{\text{probe}}(t) E_{\text{THz}}(t). \quad (1)$$

The probe beam is given by  $I_{\text{probe}}(t) = I_{\text{opt}}^0 [A + \cos(\Omega t - \varphi_2)]$ , where  $\varphi_2 = \Omega d_2 / c$  corresponds to the phase of the probe beam and varies with the optical pathlength for the probe arm  $d_2$ . In this experiment, we measure the dc component of the change in the signal  $\langle \Delta I_{\text{EO}}(t) \rangle$ , where  $\langle \cdot \rangle$  represents the time average. It follows that

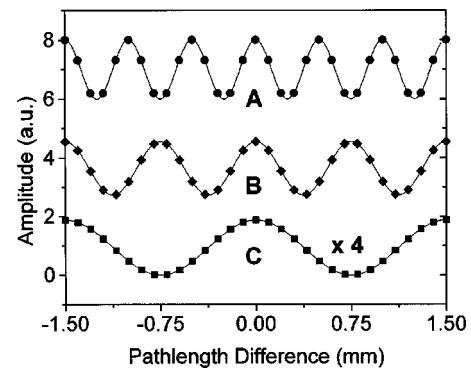


FIG. 2. Measured amplitude of the electro-optic signal vs the pathlength difference for three different frequencies: 0.6 THz (trace A), 0.4 THz (trace B), and 0.2 THz (trace C). The solid lines, calculated using Eq. (2), are the best fit to the data. The traces have been vertically offset from the origin for clarity.

$$\begin{aligned} \Delta I_{\text{EO}} &= \langle \Delta I_{\text{EO}}(t) \rangle \propto I_{\text{opt}}^0 E_T \cos[\varphi_2 - \varphi_1] \\ &= I_{\text{opt}}^0 E_T \cos[\Omega \Delta d / c], \end{aligned} \quad (2)$$

where  $\Delta d$  is the relative pathlength difference ( $= d_2 - d_1$ ). Thus, this measurement scheme yields both the amplitude and phase of the THz electric field. It may be regarded as a combination of a frequency up-conversion process and optical homodyne detection.

Figure 2 shows the measured electro-optic signal for three distinct laser beat frequencies  $\Omega$  as a function of  $\Delta d$ , the relative path-length difference between the pump and probe arms. We can infer the THz beat frequencies by measuring the distance between the peaks in the signal. These distances are approximately 0.5 mm for trace A, 0.75 mm for trace B, and 1.5 mm for trace C, which corresponds to 0.6, 0.4, and 0.2 THz, respectively [using Eq. (2)]. These values are in excellent agreement with the detuning wavelength between the two lasers: 1.5 nm (0.6 THz) for trace A, 1 nm (0.4 THz) for trace B, and 0.5 nm (0.2 THz) for trace C. The amplitude of each trace corresponds to the overall system efficiency at the corresponding frequency. It is apparent that one may easily measure the linear optical properties of a medium by measuring the change in amplitude and relative phase in  $\Delta I_{\text{EO}}$  induced by placing the test sample in the THz beamline. This has been elegantly demonstrated in Ref. 6.

We have also measured the overall response of the system as a function of THz frequency. Figure 3 shows the relative amplitude of the *electric field* of the cw THz radiation measured for various laser detuning values. These am-

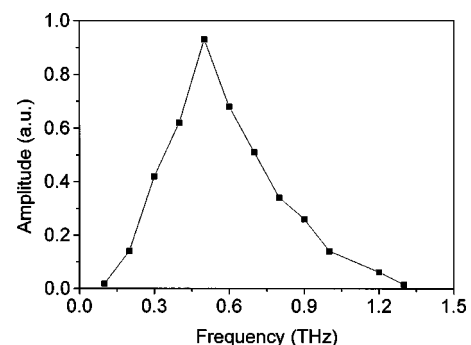


FIG. 3. System response vs THz frequency.

plitudes are normalized for the optical pump power. As one might expect, there is a resonance peak at approximately 0.5 THz associated with the resonance frequency of the dipole antenna. The response drops rapidly beyond this frequency and is strongly suppressed beyond 1.3 THz.

As stated above, in the optical scheme for the electro-optic measurements, we worked near the null point in a crossed polarizer arrangement. This configuration was used because it provided the largest fractional modulation in the probe intensity for a given THz field strength, while maintaining a linear response in the THz field.<sup>11</sup> We achieved an extinction ratio of  $\sim 100:1$ , yielding a factor of  $\sim 5$  improvement in the fractional modulation, relative to quarter-wave biasing conditions. This low extinction value is believed to arise from scattering and inhomogeneous stress-induced birefringence in the ZnTe crystal. Experimentally, the THz electric field induced a fractional modulation of  $\sim 8 \times 10^{-6}$ , which is well above the shot-noise-limited detection floor of  $\sim 10^{-8}$  (in a 1 Hz bandwidth).

In order to estimate the magnitude of the THz electric field, it is necessary to consider the effective thickness of the electro-optic crystal. Absorption of the THz radiation within the nonlinear medium plays a significant role in determining this value. If we assume uniform attenuation in passing through the ZnTe crystal, the effective thickness of the crystal is given by  $(2/\alpha)[1 - \exp(-\alpha L/2)]$ , where  $\alpha$  is the power absorption coefficient and  $L$  is the crystal thickness. For frequencies below 1 THz, the power absorption coefficient is  $\alpha \sim 2 \text{ cm}^{-1}$ ,<sup>15</sup> corresponding to an effective crystal thickness of 5 mm. Based on this interaction length, we estimate that the amplitude of the THz field at 0.5 THz was  $\sim 30 \text{ mV/cm}$ .

In the analysis above, we assumed perfect phase matching for electro-optic detection. This is not strictly valid for all of the THz frequencies shown in the data above. The coherence length for electro-optic detection<sup>14</sup> in  $\langle 110 \rangle$  ZnTe exceeds the crystal length of 6.7 mm for THz frequencies  $\leq 0.9$  THz for an optical probe wavelength of  $\sim 850 \text{ nm}$ .<sup>15</sup> For higher THz frequencies, the coherence length diminishes rapidly – 5.2 mm for 1 THz and 2.9 mm for 1.3 THz. Thus, the steep decline in response beyond  $\sim 0.9$  THz can be attributed, in part, to the reduced interaction length.

In conclusion, we have demonstrated the coherent detec-

tion of freely propagating continuous-wave THz radiation using electro-optic detection in a ZnTe crystal. An amplitude-modulated optical beam derived from the superposition of two single-frequency diode lasers is used for both the generation and detection of cw THz radiation. The electro-optic detection process may be viewed as a frequency up-conversion process coupled with optical homodyne detection, which yields favorable characteristics with respect to background suppression, as well as information on the phase of the THz electric field. The overall system is immediately amenable to high-resolution coherent spectroscopy in the far infrared. Further enhancement of the signal-to-noise ratio of the system may be possible by using optimized detection media that exhibit large optical nonlinearities and interaction lengths.

One of the authors (T.F.H.) acknowledges support from the NSF (Grant No. CHE-96-12294) and the AFOSR (Grant No. F49620-98-1-0137).

<sup>1</sup>E. R. Brown, F. W. Smith, and K. A. McIntosh, *J. Appl. Phys.* **73**, 1480 (1993).

<sup>2</sup>S. Verghese, K. A. McIntosh, and E. R. Brown, *IEEE Trans. Microwave Theory Tech.* **45**, 1301 (1997), and references therein.

<sup>3</sup>P. Chen, G. A. Blake, M. C. Gaidis, E. R. Brown, K. A. McIntosh, S. Y. Chou, M. I. Nathan, and F. Williamson, *Appl. Phys. Lett.* **71**, 1601 (1997).

<sup>4</sup>S. Matsuura, M. Tani, and K. Sakai, *Appl. Phys. Lett.* **70**, 559 (1997).

<sup>5</sup>H. Hidaka, S. Matsuura, M. Tani, and K. Sakai, *Electron. Lett.* **33**, 2039 (1997).

<sup>6</sup>S. Verghese, K. A. McIntosh, S. Calawa, W. F. DiNatale, E. K. Duerr, and K. A. Molvar, *Appl. Phys. Lett.* **73**, 3824 (1998).

<sup>7</sup>A. S. Welington and D. H. Auston, *J. Opt. Soc. Am. B* **13**, 2783 (1996).

<sup>8</sup>Q. Wu and X.-C. Zhang, *Appl. Phys. Lett.* **67**, 3523 (1995).

<sup>9</sup>P. U. Jepsen, C. Winnewisser, M. Schall, V. Schyja, S. R. Keiding, and H. Helm, *Phys. Rev. E* **53**, R3052 (1996).

<sup>10</sup>A. Nahata, D. H. Auston, T. F. Heinz, and C. Wu, *Appl. Phys. Lett.* **68**, 150 (1996).

<sup>11</sup>Z. Jiang, F. G. Sun, Q. Chen, and X.-C. Zhang, *Appl. Phys. Lett.* **74**, 1191 (1999).

<sup>12</sup>Y. Cai, I. Brener, J. Lopata, J. Wynn, L. Pfeiffer, and J. Federici, *Appl. Phys. Lett.* **71**, 2076 (1997).

<sup>13</sup>S. Gupta, M. Y. Frankel, J. A. Valdmanis, J. F. Whitaker, and G. A. Mourou, *Appl. Phys. Lett.* **59**, 3276 (1991).

<sup>14</sup>A. Nahata, A. S. Welington, and T. F. Heinz, *Appl. Phys. Lett.* **69**, 2321 (1996).

<sup>15</sup>G. Gallot, J. Zhang, R. W. McGowan, T. Jeon, and D. Grischkowsky, *Appl. Phys. Lett.* **74**, 3450 (1999).